Monitoring the *in Vivo* Delivery of Proteins from Carbomer Hydrogels by X-Ray Fluorescence

Donald S. MacLean-McDavitt,[1,4] J. David Robertson,[2] and Michael Jay[3]

Received October 25, 2002; accepted November 5, 2002

Purpose. To measure the effect of protein size on their disappearance from subcutaneously implanted carbomer hydrogel matrices.
Methods. A series of different molecular weight (MW) proteins were iodinated, incorporated into Carbopol hydrogels, injected subcutaneously into rats, and monitored using X-ray fluorescence (XRF).
Results. A 10 mg/mL minimum concentration of Carbopol-940 was necessary before protein [50 mg/mL iodinated bovine serum albumin (I-BSA)] retention times increased with increasing hydrogel concentration. The decreasing protein signal was not caused by outward protein diffusion or iodoprotein hydrolysis. As the protein MW increased, protein retention times lengthened [e.g., 6.2 h for insulin (5.7 kDa) to 13.3 h for thyroglobulin (669 kDa)]. Protein disappearance was monophasic first-order for some proteins and biphasic first-order for others. The disappearance rate constant ranged from 0.093 ± 0.005 $h^{-1/2}$ to 0.187 ± 0.057 $h^{-1/2}$, indicating gel erosion rather than protein diffusion as the rate-limiting mechanism. Entrapped I-BSA in Carbopol-1342 NF, pH 7.4, and Carbopol 2001-ETD, pH 7.4, gel matrices yielded different disappearance rates and profiles than Carbopol-940. The overall 50% disappearance rate of I-BSA was greatest for Carbopol-1342 NF (41 ± 8 h), followed by Carbopol-2001 ETD (25 ± 2 h) and Carbopol-940 (10.5 ± 0.7 h).
Conclusion. XRF is a noninvasive technique that can be used to follow the status of macromolecules *in vivo*.

KEY WORDS: protein; X-ray fluorescence (XRF); carbomer; *in vivo*; kinetics.

INTRODUCTION

An alternative method to intravenous and oral delivery of therapeutic compounds involves entrapping them within a polymeric matrix and then implanting them. Polymeric delivery systems are used to achieve a continuous administration of systemic drugs such as the contraceptive Norplant® (1). Such implants, introduced surgically into the body (*e.g.*, subcutaneously or intramuscularly), allow drugs to bypass delivery barriers and eliminate the need for repeated administrations (2). Successful sustained delivery of the therapeutic agent often depends on the nature and property of the matrix. One possible implant formulation for delivery of proteins is a hydrogel matrix (3–7).

Hydrogels are cross-linked hydrophilic polymers. Their elasticity and minimal mechanical strength result from the abundance of water in their structures. Changes in pH, temperature, ionic strength, or solvents can cause viscosity changes or the erosion of the hydrogel. Efficient delivery of entrapped macromolecules within a monolithic hydrogel matrix requires a breakdown of the matrix or large hydrogel porosity.

One class of hydrogel is the ionic polyacrylic acids, also known as carbomers or Carbopols®. These synthetic polymers have been used extensively in commercial applications (8) as thickening agents, adhesives, and suspending agents for pharmaceuticals. Carbomers are high-molecular-weight cross-linked acrylic acid-based polymers modified with C10–C30 alkyl acrylates. Their carboxyl moieties provide reliable bioadhesive and buffering properties (9,10), often used within an *in vitro* and *in vivo* delivery context. On dispersion in solution and neutralization with a base, the carbomers ionize, which results in expansion. Because of the ionic nature of carbomers, salts significantly decrease their viscosity (11,12) through hydrogen bonding alteration on the poly(acrylic acid) backbone. Homopolymers of poly(acrylic acid) above 500 Da are not easily biodegraded (13).

A major challenge of protein delivery is their *in vivo* assessment because of their inherently low serum concentration, rapid blood clearance, and enzymatic protein degradation. Two techniques most often used to assess sustained-release formulations *in vivo* require the use of fluorescent or radioactive markers in a pharmacokinetic analysis of blood and urine or, indirectly, by implant removal and subsequent analysis of the device (7,14,15). Additional quantitative techniques include enzyme–substrate concentration profiles (6), antibody production (16,17), ELISA/RIA (18,19), SDS-PAGE (7,17), and γ-scintigraphy. Radiolabels are usually used for protein distribution determination. Noninvasive techniques include γ-scintigraphy (7,20) and SPECT. Invasive techniques include organ harvesting and autoradiography, and fluorescence and cytoimmunohistochemistry are nonradiologic invasive methods. One noninvasive alternative to fluorescent and radiolabels is X-ray fluorescence (XRF) (21,22), which measures the protein clearance from the injection site.

XRF relies on the emission of X-rays by the interaction of a sample with external excitation photons. The energies of the emitted X-rays are characteristic of the elements present in the sample, and the disappearance of the fluorescence signal over time reflects the disappearance of the labeled compound(s) from the fluoresced area.

Herein we describe the utility of XRF to monitor and assess subcutaneously administered proteins (nonradioactive/nonfluorolabeled) entrapped in carbomer gels. The primary research objective was to determine the *in vivo* disappearance characteristics of various molecular weight model proteins entrapped in carbomer gels. Their 50% disappearance times and disappearance profiles are provided, along with their disappearance rate constant based on a matrix delivery device model.

MATERIALS AND METHODS

Analysis Systems

The ^{241}Am XRF sys0tem used to acquire spectra has previously been described (21,22). An area of 3.1 cm^2 is fluo-

[1] Department of Pharmaceutical Chemistry, The University of Kansas, Lawrence, Kansas 66047.
[2] Department of Chemistry, University of Missouri, Columbia, Missouri 65211.
[3] College of Pharmacy, University of Kentucky, Lexington, Kentucky 40536.
[4] To whom correspondence should be addressed. (e-mail: dmaclean@ku.edu)

0724-8741/03/0300-0435/0 © 2003 Plenum Publishing Corporation

resced at 2.0 cm from the source holder, yielding qualitative and quantitative elemental information without any spatial distribution information.

γ-Scintigraphy (Siemens, Germany) was used under the following conditions: a low-energy lead collimator with the lower energy threshold set at zero. Static 5-min measurements were taken over a 4-day period. The resolution was 5 mm for [^{125}I]BSA at approximately 6 inches.

Protein Labeling

The following proteins (Sigma, St. Louis, Missouri) were iodinated: insulin (bovine), α-lactalbumin (bovine), β-lactoglobulin (bovine), phosvitin (egg yolk), α-amylase (*Bacillus* species), serum albumin (bovine), concanavalin A (*C. ensiformis*), β-galactosidase (*A. oryzae*), β-glucosidase (almonds), alcohol dehydrogenase (yeast), immunoglobulin G (bovine), glucose oxidase (*A. niger*), amyloglucosidase (*Rhizopus*), and thyroglobulin (bovine).

The proteins were dissolved in phosphate-buffered saline (PBS), pH 7.4. Sodium iodide or potassium iodide (Aldrich) was first added, followed by chloramine-T (22), and the reaction was allowed to proceed for approximately 1 h, after which it was terminated using sodium metabisulfite (Aldrich). Initially, labeled BSA was purified using a preequilibrated Sephadex G-50 (cross-linked Dextran) (Pharmacia, Sweden) size-exclusion column. Sodium azide (Aldrich) was flushed through the column to prevent bacterial growth. The void volume was determined using Blue Dextran (Sigma). Insulin, lysozyme, α-lactalbumin, bovine serum albumin (BSA), and thyroglobulin were used as molecular mass calibrators (all compounds from Sigma). The protein elute fractions were consolidated into a round-bottom flask, lyophilized, weighed, and analyzed for halogen content by XRF. The collected protein powder was stored at 4°C in scintillation vials. After the proof of concept stage for iodinating BSA, ultrafiltration (Pall Filtron, Northbough, MA) replaced size exclusion chromatography as the protein purification method.

For the γ-scintigraphy experiments, BSA was dissolved in PBS, pH 7.4, followed by the addition of ^{125}I-labeled sodium iodide (ICN, Costa Mesa, CA) and Iodobeads ™ (Pierce). The reaction was halted after 5 min by the removal of the Iodobeads. The mixture was purified by ultrafiltration and then lyophilized.

The lyophilized labeled proteins were assayed for molecular mass using Sephadex G-25, G-50, and G-200 size-exclusion chromatography. Molecular mass calibration was done by using polymyxin, bacitracin B sulfate, vancomycin hydrochloride, insulin, lysozyme, myoglobin, α-lactalbumin, BSA, and thyroglobulin (all from Sigma). Protein or peptide elution periods were determined by UV-vis spectroscopy at 280 nm, by the Lowry assay (Sigma) (e.g., bacitracin), or through fluorescence with excitation at 360 nm and emission at 450 nm (e.g., polymyxin).

Hydrogel Matrix Preparation and Protein Loading

Stock gels of Carbopol-940, Carbopol-1342 NF, and Carbopol-2001 ETD (B.F. Goodrich, Cleveland, Ohio) at twice their final concentrations were prepared by dissolving the dried powder in PBS, pH 7.4. Ammonium hydroxide (NH_4OH) was added to neutralize excess acidity and to bring the pH back to 7.4. Once the gels were homogeneous and at the appropriate pH, PBS was added until the proper concentrations were achieved. Stock gels that reached 3 months of age were replaced with freshly prepared gels.

Iodinated BSA (I-BSA) (50.0 mg/mL) was immersed in Carbopol-940 gels, pH 7.4 (0.0 mg/mL to 19.0 mg/mL), allowed to partition and penetrate the hydrogel, and then mixed by hand to obtain a homogeneous gel. As a free-iodide control, potassium iodide (4.57 mg/mL) was added to 14.1 mg/mL Carbopol-940, pH 7.4, to obtain an iodide concentration equivalent to I-BSA. Non-I-BSA proteins (25.0 or 50.0 mg/mL) were incorporated into stock Carbopol-940 gels (14.1 mg/mL, pH 7.4) and allowed to penetrate into the gel matrix. PBS was subsequently added, and the matrix was hand mixed to obtain a monolithic gel. In addition, I-BSA (50.0 mg/mL) was also entrapped into 14.1 mg/mL, pH 7.4, Carbopol-1342 NF and Carbopol-2001 ETD gels using the same procedure as Carbopol-940. Every protein/hydrogel was done in triplicate or greater.

Formulation Administration and Data Collection

Retired female Sprague–Dawley breeder rats (Harlan Sprague Dawley, Inc., Indianapolis, Indiana) were used. The rats were placed in an atmosphere containing ethyl ether and then anesthetized with 0.25 mL of 1:10 acepromazine–ketamine given intramuscularly (IM) in the thigh with 0.50 mL of 1:10 pentobarbital–saline intraperitoneally (IP), if needed. After the rats were fully anesthetized, the dorsal hair on the opposite side was clipped, and the rats were secured onto a plastic platform and placed underneath the X-ray source for a 5-min background measurement. The rats were then removed from under the source and given subcutaneous (SC) injections of hydrogel–protein formulation at the clipped site. The location of the resulting welt was outlined with a marker. The rats were again placed under the X-ray source, and their skin was marked to allow for consistent repositioning. A series of 5-min XRF measurements were collected for 24 to 96 h after the SC injection. Between measurements, the rats were placed in their cages and allowed food and water *ad libitum*. The initial background spectrum was subtracted from each successive XRF measurement (Fig. 1). A region of interest was set on each subtracted measurement to quantify the X-rays from the reporter atom. The dead time (minimum amount of time separation that must separate two events in order to be recorded as two separate events) of each rat was constant; therefore, no dead-time corrections were needed.

Mathematical Modeling

Analyses of experimental data were carried out using the X-ray yield from the iodine reporter atom (or from decay-corrected γ-ray emissions when ^{125}I labels were used). Four phenomenologic equations were used to characterize the protein disappearance. Matrix-controlled processes were fit to the following empiric equation (10,23):

$$M_t/M_\infty = C\,t^n \quad (M_t/M_\infty < 0.6) \tag{1}$$

where M_t is the cumulative amount of protein released by time t, M_∞ is the amount of protein originally present in the gel, M_t/M_∞ represents the fraction of the total protein de-

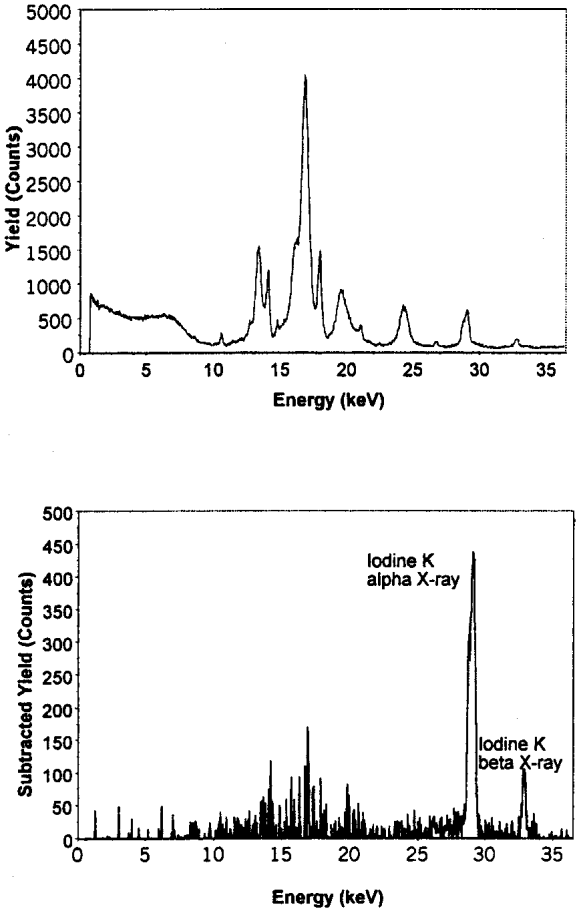

Fig. 1. (Top) The X-ray fluorescence spectrum for iodinated bovine serum albumin in Carbopol-940 taken for 5 min after injection. **(Bottom)** The background-corrected spectrum for iodinated bovine serum albumin in Carbopol-940. The 28.6-keV iodine K α and the 32.3-keV K β peaks are now clearly visible.

creased at time t, C is the diffusion constant and n is the disappearance index that characterizes the mode of protein transportation. The diffusion coefficients of the protein in the hydrogel were calculated using Eq. (2), assuming n = 0.5 (24).

$$M_t/M_\infty = 4(D_m/\pi h^2)^{0.5}\,(t)^{0.5} \quad (2)$$

where M_t is the cumulative amount of protein released by time t, M_∞ is the amount of protein originally present in the gel, D_m is the diffusion coefficient of the protein in the matrix, and h is the thickness of the hydrogel. The disappearance rate constant is defined as $R = 4(D_m/\pi h^2)^{0.5}$.

In addition, each disappearance profile was analyzed for monophasic and biphasic disappearance characteristics. For a first-order monophasic profile, Eq. (3) was used to fit data, whereas biphasic profiles were fit to Eq. (4). The results are reported as 50% disappearance (T_{50}), not half-life.

$$M_t = M_0 \exp(-kt) \quad (3)$$

where M_t is the amount of protein at time t, M_0 is the original amount of protein injected at the fluoresced site, and k is the first-order disappearance constant,

$$M_t = A \exp(-at) + B \exp(-bt) \quad (4)$$

where M_t is the amount of protein at time t, a and b are the rate coefficients for the two phases, A is the zero-time intercept for the first phase, and B is the zero-time intercept for the second phase. The extrapolated value of the longer-disappearance second component subtracted to yield the disappearance curve for the first-component curve.

RESULTS

Effect of Carbopol-940 Concentration

The top portion of Fig. 1 shows a representative spectrum of I-BSA in Carbopol-940 gel, and the bottom portion shows the background-corrected spectrum. First-order disappearance profiles were seen for I-BSA in Carbopol-940 hydrogels with polymer concentrations ranging from 0 to 19.0 mg/mL Carbopol-940 (Fig. 2). A minimum of 10 mg/mL Carbopol-940 was required before 50% disappearance (T_{50}) times began increasing (Fig. 3). Minimum T_{50} was seen at 0 mg/mL Carbopol-940 with a $T_{50} = 6.5 \pm 0.2\ h^{-1/2}$ and a disappearance rate constant $= 0.227 \pm 0.014\ h^{-}$. Maximum T_{50} was seen at 19.0 mg/mL Carbopol-940 with a $T_{50} = 14.0 \pm 0.5$ h and a disappearance rate constant $= 0.144 \pm 0.015 h^{-1/2}$ (Table I). Free iodide entrapped in 14.1 mg/mL carbopol-940 had a 13.4 ± 0.7 min half-life.

Protein's Fate

γ-Scintigraphy was used to monitor the BSA disappearance over the 4 days following the injection (Table II). No lateral diffusion was evident (data not shown). The disappearance of the [^{125}I]BSA from the injection site followed first-order kinetics. The half-life was 16.7 ± 0.56 h ($n = 1$). The whole-body half-life was 31.8 h. The labeled protein migrated to the liver, where the ^{125}I activity first increased, then began to decrease over the measurement period. The ^{125}I activity in the thyroid increased with time and reached a maximum of 4% by day 2.

Effect of Protein Size

Various iodinated proteins (50.0 mg/mL final concentration) were substituted for I-BSA to determine the effect of protein mass on the disappearance rates from 14.1 mg/mL

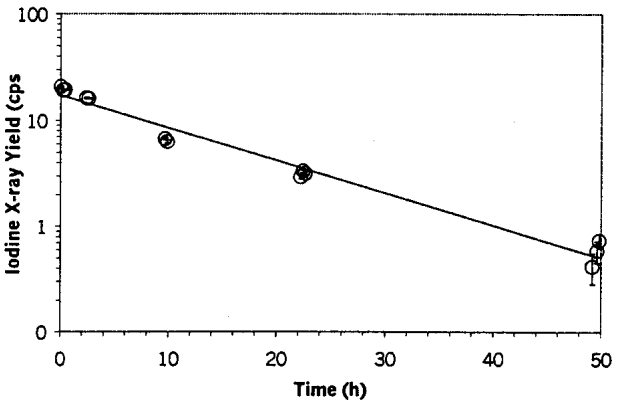

Fig. 2. An I-BSA disappearance profile after subcutaneous injection of 50.0 mg/mL I-BSA in 14.14 mg/mL Carbopol-940.

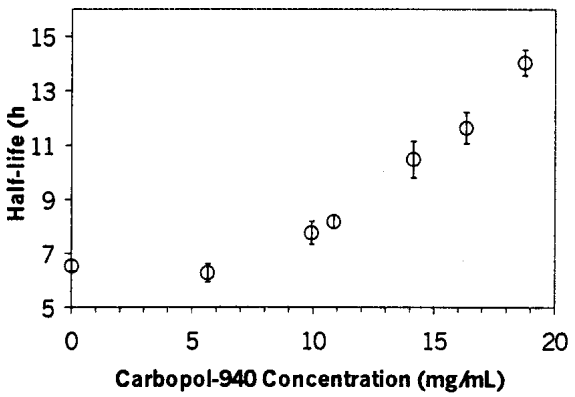

Fig. 3. Variation in the 50% disappearance of I-BSA with varying concentrations of Carbopol-940. The I-BSA concentration was 50.0 mg/mL in all cases. Once a threshold concentration was achieved, as the concentration increased, the retention time increased.

Carbopol-940, pH 7.4, hydrogels. A comparison of the 50% disappearance times for proteins exhibiting monophasic and biphasic disappearance kinetics is shown in Fig. 4a. The retention time increased as the molecular mass increased for the monophasic proteins. For the proteins that followed biphasic disappearance, the 50% disappearance time was greater than those of monophasic proteins of comparable mass. When the extrapolated second component was subtracted from the overall profile, the T_{50}s for the first components were comparable to the overall T_{50} of monophasic proteins of equivalent mass (Fig. 4b, Table III). The overall T_{50} ranged from 8.0 ± 1.0 to 43 ± 11 h. The disappearance rate constant for the proteins ranged from 0.093 ± 0.005 $h^{-½}$ to 0.187 ± 0.057 $h^{-½}$ (Table III).

Effect of Protein Load

Iodinated β-lactoglobulin (I-β-lactoglobulin, 17.5 kDa), 25.0 and 50.0 mg/mL, or I-BSA (66 kDa) incorporated into 14.1 mg/mL Carbopol-940 gels, pH 7.4, showed no concentration–retention time dependence as determined by the two-sided Student *t* test ($\alpha = 0.05$). The T_{50}s for 25.0 and 50.0 mg/mL I-β-lactoglobulin were 7.9 ± 0.3 h ($n = 4$) and 8.0 ± 1.0 h ($n = 6$), respectively. The T_{50}s for 25.0 and 50.0 mg/mL I-BSA were 10.0 ± 1.4 h ($n = 5$) and 10.5 ± 0.7 h ($n = 6$), respectively.

Table I. The Disappearance Rate Constant, R, for 50.0 mg/mL I-BSA in 14.14 mg/mL Carbopol 1342 NF and Carbopol 2001 ETD and Various Concentrations of Carbopol-940

Hydrogel condition	Disappearance rate constant ($h^{-1/2}$)	Replicates
14.14 mg/mL Carbopol-1342 NF	0.090 ± 0.011	6
14.14 mg/mL Carbopol-2001 ETD	0.105 ± 0.031	7
pH 7.4 PBS	0.227 ± 0.014	6
5.61 mg/mL Carbopol-940	0.204 ± 0.018	5
9.93 mg/mL Carbopol-940	0.197 ± 0.003	3
14.14 mg/mL Carbopol-940	0.158 ± 0.044	6
14.77 mg/mL Carbopol-940	0.188 ± 0.018	3
16.33 mg/mL Carbopol-940	0.164 ± 0.024	8
18.75 mg/mL Carbopol-940	0.144 ± 0.015	7

Table II. Body Distribution of ^{125}I-Labeled BSA[a]

Time after injection	Distribution of ^{125}I activity (%)			
	Whole body	Injection site	Liver	Thyroid
0 h	100.0	95.8	0.6	0.2
0.3 h	90.4	86.2	0.6	0.2
1 h	97.9	92.6	1.0	0.3
2 h	102.1	96.3	1.1	0.3
3 h	100.8	94.4	1.3	0.3
15 h	86.9	69.6	5.0	1.8
2 d	36.0	15.1	6.1	4.1
3 d	20.8	4.9	3.6	4.0
4 d	15.5	2.7	2.3	3.6

[a] γ-Scintigraphy indicated that the bulk of the activity does not persist within the body. The activity builds to a zenith in the liver at approximately 15 h at 5% of the original dose and then slowly declines. The activity in the thyroid, related to free iodide, crests later at 4% and subsides more slowly than in the liver.

Carbopol-1342 NF and Carbopol-2001 EDT Gels

Figure 5 shows the disappearance of I-BSA from three types of carbomer formulations at the same protein and polymer concentrations (50.0 mg/mL I-BSA and 14.1 mg/mL Carbopols, pH 7.4). Previously, it was shown that I-BSA in Car-

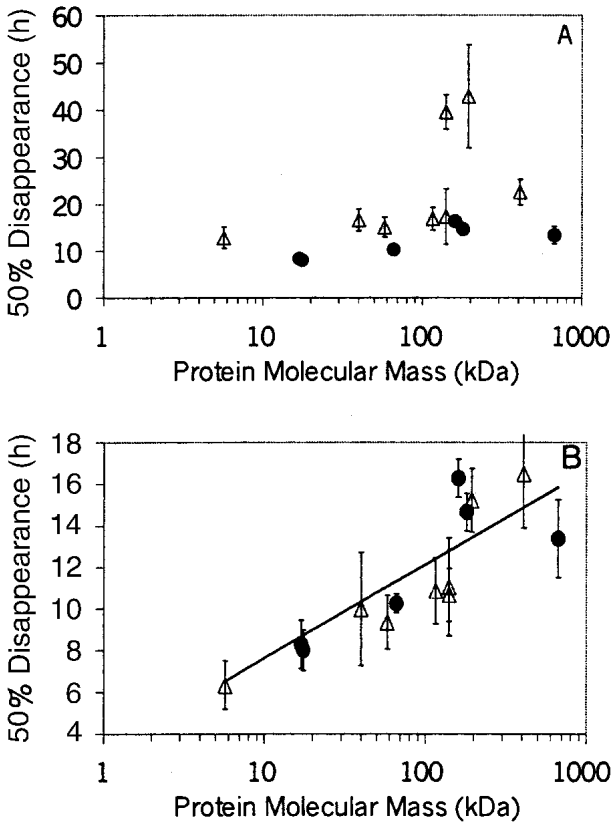

Fig. 4. (A) Overlay plot of monophasic and biphasic proteins in 14.14 mg/mL Carbopol-940. The biphasic proteins had longer overall 50% disappearance times than monophasic proteins of comparable molecular mass. (B) Overlay of 50% disappearance times for proteins that followed monophasic disappearance and the first component of those that followed biphasic disappearance.

Table III. The 50% Disappearance Times (T_{50}) and Disappearance Rate Constants (R) for 50.0 mg/mL Proteins in 14.14 mg/mL Carbopol-940, pH 7.4

Protein	M.W. (kDa)[a]	pI[a]	Components	T_{50}^{a} overall (h)	T_{50}^{a} first component (h)	Replicates	Disappearance rate constant ($h^{-1/2}$)
I-insulin	5.7	5.32	2	12.9 ± 2.3	6.3 ± 1.2	10	0.145 ± 0.027
I-α-Lactalbumin	14.2	5.01	1	8.3 ± 1.2	NA[a]	5	0.179 ± 0.018
I-β-Lactoglobulin	17.5	5.2	1	8.0 ± 1.0	NA	6	0.187 ± 0.057
I-Phosvitin	40	3.8–4.1	2	16.6 ± 2.3	10.0 ± 2.7	4	0.132 ± 0.004
I-α-Amylase	58	8.7	2	15.1 ± 2.2	9.4 ± 1.3	6	0.142 ± 0.013
I-Bovine serum albumin	66	4.9	1	10.5 ± 0.7	NA	6	0.158 ± 0.044
I–β-Galactosidase	116	4.5	2	16.8 ± 2.4	10.9 ± 1.6	4	0.140 ± 0.011
I-β-Glucosidase	140	4.46	2	39.5 ± 3.7	10.7 ± 1.3	5	0.093 ± 0.005
I-Alcohol dehydrogenase	140	5.4	2	17.4 ± 5.9	11.1 ± 2.4	4	0.128 ± 0.028
I-Immunoglobulin G	160	5.8–7.3	1	16.3 ± 0.9	NA	2	0.140 ± 0.001
I-Glucose oxidase	180	4.2	1	14.7 ± 0.9	NA	5	0.135 ± 0.002
I-Amyloglucosidase	194	4.6	2	42.8 ± 11.0	15.2 ± 1.5	4	0.094 ± 0.017
I-Concanavalin A	408+	5.05	2	22.6 ± 2.7	16.5 ± 2.6	6	0.101 ± 0.004
I-Thyroglobulin	669	4.5	1	13.4 ± 1.9	NA	7	0.137 ± 0.007

[a] MW, molecular mass; pI, isoelectric point; T_{50}, time for 50% disappearance; NA, not applicable.

bopol-940 followed monophasic, first-order kinetics with the 50% disappearance of 10.5 ± 0.7 h ($n = 6$). In Carbopol-1342 NF, I-BSA exhibited biphasic disappearance with an overall T_{50} of 44 ± 14 h ($n = 6$) and a first component T_{50} of 15 ± 5 h ($n = 6$). The age of the formulation did not affect the disappearance profile. In Carbopol-2001 EDT, I-BSA exhibited both monophasic and biphasic disappearance. In freshly prepared I-BSA–Carbopol-2001 EDT gels, I-BSA followed a monophasic profile with a T_{50} of 25 ± 2 h ($n = 3$). In 10-day-old formulations, I-BSA exhibited biphasic disappearance with a first component T_{50} of 15.8 ± 0.8 h ($n = 3$) and an overall T_{50} of 24 ± 3 h ($n = 3$). The overall group mean T_{50} was 25 ± 2 h ($n = 6$).

DISCUSSION

A 10 mg/mL Carbopol-940 threshold was required before I-BSA retention began to increase (22). This may reflect retardation of I-BSA diffusion from greater gel viscosity, greater polymer–protein interactions, or decreasing carbomer porosity. The 14.1 mg/mL Carbopol concentration was chosen as the matrix concentration for comparative studies because it could increase the retention time of I-BSA (10.5 ± 0.7 h half-life) over PBS (6.5 ± 0.2 h half-life) and still remain injectable. Free iodide at the same iodide concentration disappeared with a 13.4 ± 0.7 min half-life (22). This indicates that the I-BSA signal decline was from the disappearance of labeled protein, not from unattached iodine as a result of incomplete purification. Furthermore, γ-scintigraphy indicated that lateral diffusion of the protein was not the responsible for the decreasing iodine X-ray yield seen from the XRF measurements. In addition, γ-scintigraphy showed that I-BSA accumulates in the liver, whereas free iodine (iodide released through hydrolysis of the protein–iodide bond) accumulates in the thyroid. This amount never exceeded 4% of the total iodine administered.

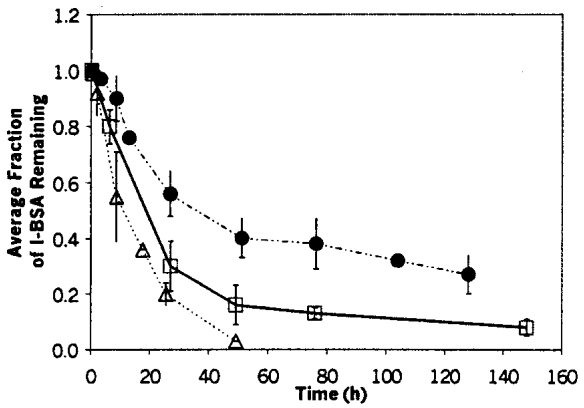

Fig. 5. Overlay plot for the disappearance of I-BSA in the three types of Carbopol: Carbopol-1342 NF (●), Carbopol-2001 ETD (□), and Carbopol-940 (△).

Other iodinated proteins (all at 50 mg/mL) were entrapped at the same Carbopol concentration (14.1 mg/mL) to determine the effect of protein size on disappearance rates. Some proteins followed monophasic first-order kinetics, whereas others demonstrated biphasic disappearance profiles. Although there was no clear explanation for these observations, possible reasons for the differences in the disappearance rate and the phasic nature include the dual clearance pathway for proteins (23,25), protein interactions, porosity of the matrix, polymer erosion, protein size, and protein concentration gradient. Our results concur with observations made by numerous authors showing a similar relationship between size and rate for macromolecules when entrapped within a matrix (3,23,26,27). Our study showed a logarithmic relationship between the 50% disappearance rate and the mass of the protein.

Because only buffer salts were used during protein lyophilization in order to obtain the purest labeled protein, the likelihood of protein subunit dissociation, dimerization, or aggregation was enhanced (28). This was evident with iodinated β-lactoglobulin when size-exclusion chromatography demonstrated that 17.5-kDa subunits, not the 35-kDa protein, existed. Additionally, because of the matrix pH, Concanavalin A was treated as a tetrameric protein. The biphasic first-order and occasional monophasic first-order insulin disappearance phenomenon was probably a result of insulin ag-

gregation. Unfortunately, insulin structure after gel incorporation was not determined at the time of the experiments.

Protein disappearance rates/profiles can be affected by hydrogen bonding (9,29). An attempt using polytyrosines of different lengths to circumvent this concern was not attainable. It is noteworthy, however, that the isoelectric points (pI) of the majority of proteins used possessed a pI near 5 before labeling and would change only slightly on iodination (Table III). Additionally, varying the salt concentration was not useful because salt lowers carbomer viscosity (12) and can influence protein disappearance. Changing carbomer composition, however, resulted in changes in I-BSA retention times when all other factors remained constant (Fig. 5). Viscosity cannot be the sole factor because Carbopol-1342 NF and Carbopol-2001 ETD viscosities were equal to or less than that of Carbopol-940 (9,11). A possible reason for the viscosity–retention discrepancy is cross-linking and backbone structural differences among the carbomers leading to different rates of gel deterioration (29), protein–carbomer interactions, porosity, and potential protein aggregation. This is suggested by the monophasic disappearance of I-BSA from Carbopol-940, biphasic disappearance from Carbopol-1342 NF, and dual phases from Carbopol 2001 ETD gels. Protein–polymer interactions were not studied using biophysical techniques.

Another possibility for the differences in disappearance rates among the proteins used (entrapped at 50.0 mg/mL) is a protein concentration gradient. Smaller proteins would have a greater molar concentration gradient than those of larger molecular mass. If the disappearance rate was molar concentration-dependent, the larger molar concentration would deliver the protein faster, assuming no protein–protein interactions. To examine this possibility, I-BSA and I-β-lactoglobulin at two concentrations were used. The Student *t* test ($\alpha = 0.05$) indicates there was no protein molar concentration dependence with I-BSA or I-β-lactoglobulin dispersal. This may indicate that the disappearance of these proteins incorporated into 14.14 mg/mL Carbopol-940 is controlled by gel erosion. A noteworthy observation is that the largest protein disappearance rate constant was two times greater than that of the smallest protein (0.187 ± 0.057 vs. 0.094 ± 0.077) even though the molar concentration of the smallest protein was at least 50-fold greater than that of the largest protein. One would conclude that the rate-limiting process for I-BSA disappearance from Carbopol-940 gel occurs through the breakdown of the carbomer matrix (10). The proteins did not follow Fickian or non-Fickian diffusion.

CONCLUSIONS

Previously we showed XRF's utility as a method to monitor the *in vivo* disappearance of I-BSA from a Carbopol-940 hydrogel (22). Here we expanded our previous work with numerous model proteins to assess the protein mass–disappearance rate relationship. Furthermore, two other commercially available carbomers were incorporated as matrices to determine their retention capabilities on the model protein I-BSA. Factors that influence disappearance rates were hydrogel concentration, hydrogel composition, and protein mass. Temperature, solvent, pH, and ionic strength were not factors because these did not fluctuate during the experiments.

REFERENCES

1. P. F. Harrison and A. Rosenfield. Research introduction, and use: Advancing from Norplant. *Contraception* **58**:323–334 (1998).
2. J. L. Cleland. Protein delivery from biodegradable microspheres. *Pharm. Biotechnol.* **10**:1–43 (1997).
3. P. Caliceti, F. Veronese, O. Schiavon, S. Lora, and M. Carenza. Controlled release of proteins and peptides from hydrogels synthesized by gamma ray-induced polymerization. *Farmaco* **47**:275–286 (1992).
4. H. Tanaka, M. Matsumura, and I. A. Veliky. Diffusion characteristics of substrates in Ca-alginate gel beads. *Biotech. Bioeng.* **26**:53–58 (1994).
5. W. R. Gombotz and S. F. Wee. Protein release from alginate matrices. *Adv. Drug Deliv. Rev.* **31**:267–285 (1998).
6. J. M. Barichello, M. Morishita, K. Takayama, and T. Nagai. Absorption of insulin from Pluronic F-127 gels following subcutaneous administration in rats. *Int. J. Pharm.* **184**:189–198 (1999).
7. G. L. Yewey, E. G. Duysen, S. M. Cox, and R. L. Dunn. Delivery of proteins from a controlled release injectable implant. *Pharm. Biotech.* **10**:93–97 (1997).
8. Bulletin PH-4 (US). Carbopol resin references in the 1993 *Physicians' Desk Reference*, B. F. Goodrich, Cleveland, Ohio, 1993.
9. H. Park and J. R. Robinson. Mechanisms of mucoadhesion of poly(acrylic acid) hydrogels. *Pharm. Res.* **4**:457–464 (1987).
10. N. A. Peppas, P. Bures, W. Leobandung, and H. Ichikawa. Hydrogels in pharmaceutical formulations. *Eur. J. Pharm. Biopharm.* **50**:27–46 (2000).
11. *Carbopol Water-Soluble Resins Technical Bulletin GC-67*, The B.F. Goodrich Company Specialty Chemicals, Cleveland, Ohio 44141-3247.
12. P. B. Testa and J. C. Etter. Apport de la rhéologie à l'étude des interactions entre les macromolécules de Carbopol® ainsi qu'à la détermination semi-quantitative de la force ionique de leur dispersions. *Pharm. Acta Helv.* **48**:378–388 (1973).
13. F. Kawai. Bacterial degradation of acrylic oligomers and polymers. *Appl. Microbiol. Biotechnol.* **39**:382–385 (1993).
14. Y. Yamasaki, K. Sumimoto, M. Nishikawa, F. Yamashita, K. Yamaoka, M. Hashida, and Y. Takakura. Pharmacokinetic analysis of *in vivo* disposition of succinylated proteins targeted to liver nonparenchymal cells via scavenger receptors: importance of molecular size and negative charge density for *in vivo* recognition by receptors. *J. Pharmacol. Exp. Ther.* **301**:467–477 (2002).
15. K. H. Sprugel, J. M. McPherson, A. W. Clowes, and R. Ross. Effects of growth factors *in vivo* I. Cell ingrowth into porous subcutaneous chambers. *Am. J. Pathol.* **129**:601–613 (1987).
16. M. TobÍo, J. Nolley, Y. Guo, J. McIver, and M.J. Aloso. A novel system based on a Poloxamer / PLGA blend as a tetanus toxoid delivery vehicle. *Pharm. Res.* **16**:682–688 (1999).
17. S. Cohen, H. Bernstein, C. Hewes, M. Chow, and R. Langer. The pharmacokinetics of, and humoral responses to, antigen delivered by microencapsulated liposomes. *Proc. Natl. Acad. Sci. USA* **88**:10440–10444 (1991).
18. A. Plum, H. Agersø, and L. Andersen. Pharmacokinetics of the rapid-acting insulin analog, insulin aspart, in rats, dogs, and pigs, and pharmacodynamics of insulin aspart in pigs. *Drug Metab. Dispo.* **28**:155–160 (2000).
19. T. Morita, Y. Sakamura, Y. Horikiri, T. Suzuki, and H. Yoshino. Evaluation of *in vivo* release characteristics of protein-loaded biodedegradable microspheres in rats and severe combined immunodificiency disease mice. *J. Control. Release* **73**:213–221 (2001).
20. H. J. Lee and W. M. Pardridge. Pharmacokinetics and delivery of Tat and Tat-protein conjugates to tissues *in vivo*. *Bioconjug. Chem.* **12**:995–999 (2001).
21. J. D. Robertson, E. Ferguson, M. Jay, and D. J. Stalker. Noninvasive *in vivo* percutaneous absorption measurements using X-ray florescence. *Pharm. Res.* **9**:1410–1414 (1992).
22. D. S. MacLean, J. D. Robertson, M. Jay, and D. J. Stalker. Noninvasive measurement of protein release from subcutaneous depo formulations *in vivo* using X-ray fluorescence. *J. Control. Release* **34**:167–173 (1995).
23. R. Langer and J. Folkman. Polymers for the sustained release of proteins and other macromolecules. *Nature* **263**:797–800 (1976).
24. M. T. am Ende and A. G. Mikos. Diffusion-controlled delivery of

proteins from hydrogels and other hydrophilic systems. *Pharm. Biotech.* **10**:139–165 (1992).

25. J. M. Barnes, and J. Trueta. Absorption of bacteria, toxins and snake venoms from the tissues. *Lancet* **1**:623–626 (1941).
26. D. Marshak and D. Liu (eds.) *Proteins Formulation, Delivery, and Targeting, Current Communication in Molecular Biology*, Cold Spring Harbor Laboratory, New York, 1989.
27. A. Kikuchi, M. Kawabuchi, A. Watanabe, M. Sugihara, Y. Sakurai, and T. Okano. Effect of Ca^{2+}-alginate gel dissolution on release of dextran with different molecular weights. *J. Control Release* **58**:21–28 (1999).
28. S. Sato, C. D. Ebert, and S. W. Kim. Prevention of insulin self-association and surface adsorption. *J. Pharm. Sci.* **72**:228–232 (1983).
29. M.T. am Ende and N. A. Peppas. FTIR spectroscopic investigations and modeling of solute / polymer interactions in the hydrate state. *J. Biomater. Sci. Polymer Edn.* **10**:1289–1302 (1999).
30. P. G. Righetti and T. Caravaggio. Isoelectric points and molecular weights of proteins. A table. *J. Chromatogr.* **127**:1–28 (1976).